LA-UR-19-29886
Approved for public release; distribution is unlimited.

Title: LDRD 20190608ER: DIAGNOSING NEAR-FUTURE CHANGES IN ARCTIC SEA ICE AND OCEAN CONDITIONS

Author(s): Hunke, Elizabeth Clare
Roberts, Andrew Frank
D'Angelo, Gennaro
Verma, Tarun
Chen, Min
Dann, Julian Benjamin
Urrego Blanco, Jorge Rolando
Wilson, Cathy Jean
Urban, Nathan Mark
Maltrud, Mathew Einar

Intended for: Report

Issued: 2019-09-30

LDRD 20190608ER:
DIAGNOSING NEAR-FUTURE CHANGES IN ARCTIC SEA ICE AND OCEAN CONDITIONS

E. HUNKE[1], A. ROBERTS[1], G. D'ANGELO[1], T. VERMA[2], M. CHEN[3], J. DANN[3], J. URREGO BLANCO[2,4], C. WILSON[3], N. URBAN[2], AND M. MALTRUD[1]

1. Executive Summary

Environmental changes in the Arctic present opportunities and increased hazards as potential shipping corridors open. We apply novel statistical techniques to simultaneously characterize multiple physical properties and uncertainties relevant for Arctic shipping, analyzing existing model projections to understand the likelihood of encountering high wind and low ice conditions along potential transportation routes through the Arctic Ocean. We assess the quality of Department of Energy (DOE) simulations against observed data, for these purposes. We find that the Arctic system is highly variable, but its large-scale patterns are captured by the models, allowing us to consider the two major shipping routes along Arctic coasts: the Northern Sea Route on the Russian side of the Arctic Ocean, and the Northwest Passage through the Canadian Arctic Archipelago. Our work highlights the usefulness and promise of DOE's new modeling system (E3SM) as well as limitations of the models and observed data, such as resolution, differing types of information available from models and measurements, and challenges for quantifying uncertainty and bias. A procedure developed to increase predictability in Community Earth System Model simulations could be beneficial for E3SM. This research provides insight into Arctic trends and a baseline to articulate future model development needs.

2. Introduction

Arctic warming is affecting US national interests in the Arctic, including defense operations, resource management, trade routes, and energy infrastructure [5, 18]. Transitions occurring in Arctic sea ice cover are unprecedented in the last 1450 years [15] and expanding Arctic Ocean sovereign claims complicate the US response to sea ice and ocean hydrographic changes, which affect surface and submarine operations by the U.S., allies and potential adversaries. Quantifying spatial and temporal distributions of future Arctic conditions and seasonal sea ice coverage is necessary to enhance the US national security and economic posture in the Arctic [13]. By analyzing a diverse set of Earth system simulations to characterize physical properties and uncertainties relevant to Arctic Ocean hazardous conditions in potential shipping corridors, this work provides a comparison and baseline of existing modeling capabilities for Arctic transportation needs.

Date: September 30, 2019. LA-UR-2019-

[1]T Division, Los Alamos National Laboratory, Los Alamos, NM
[2]CCS Division, Los Alamos National Laboratory, Los Alamos, NM
[3]EES Division, Los Alamos National Laboratory, Los Alamos, NM
[4]Shell Trading Services Co., Houston, TX

.

This project uses several different climate models to examine the statistics of sea ice concentration, thickness, and wind speed. Analysis tools include statistical analyses of individual variables, skill scores to quantify model skill and bias in relation to observed data, and probabilities for the simultaneous occurrence of sea ice and atmospheric conditions conducive to infrastructure icing in areas of navigable sea ice conditions. Available simulation ensembles include scenarios such as preindustrial conditions, historical runs for 1950-2014, and increasing CO_2 projections. Our access to output from multiple models with very different configurations enables assessment of the range of variability accessible in the models. This project provides guidance for many Arctic-relevant model development efforts underway in the community, e.g. [3].

The feasibility of navigation in the Arctic environment strongly depends on the safety of operations of given ship types. Besides the type of vessels, safety is affected by sea ice conditions, as well as ocean waves and currents, and on atmospheric conditions such as wind and air temperature. Previous studies of Arctic navigability have used the Arctic Transport Accessibility Model [23, ATAM] to calculate ship speed and sailing times across the Arctic. These studies assume that sea ice is the primary factor impacting speed and sailing time. ATAM uses the concept of Ice Numeral (IN) as a guide to determine whether conditions are hazardous. The IN is computed as the sum of the fractional areas of different ice types multiplied by Ice Multipliers for each of those ice types, which depend on the ice types and different ship classes. Typically, the Ice Multipliers are functions only of sea ice concentration and thickness, and of ship type. However, a better description of navigability in iced environments should also consider ice roughness and decay (which affect strength), and waves. If wave data is not available, previous studies an have used wind speed as a proxy for significant wave height with a quadratic dependency. Higher winds and waves, combined with subzero air temperatures, may also increase the danger of sea spray deposition on ship superstructures (rime icing), which increases risk for ships in the Arctic [20].

We examine statistics of sea ice concentration, thickness, and wind speed during the extended navigation season here defined between June to September. While statistical analysis is straight forward for individual variables, a more appropriate approach considers the simultaneous occurrence of critical values of these variables. We compute simultaneous exceedance probabilities of certain conditions that make navigation unsafe and present a selection of representative results. For basic comparisons and to build the statistics necessary for multivariate analysis, we calculate simple minimum, mean and maximum values, standard deviation and correlation between data sets, and we evaluate bias in comparison with observations. Taylor diagrams [24], which simultaneously account for correlation, root-mean-square difference, and variance ratio, are used to compare output from several climate models against observations of ice thickness.

3. Multivariate statistical approach

The multidimensional representation of joint distributions of relevant variables for Arctic shipping is based on the concept of statistical copulas [21]. Given a random set of random variables (e.g. sea ice concentration, thickness, wind speed, etc.), the copula approach provides a statistically rigorous emulation of a data set which might not have enough data points for direct statistical analysis. Estimation of the joint distribution involves finding a suitable multi-dimensional representation of (possibly) correlated data, in two stages. First, the marginal univariate distributions for each individual variable are found, and the best statistical model to represent them is chosen from goodness-of-fit (gof) tests. We used the R package *fitdistrplus*, which supports a number of probability distributions. The second step fits a copula using the data and the marginal distributions obtained in the first step.

4. Data

We analyze Arctic sea ice concentration and thickness, with wind speed later included in the copula analysis.

4.1. **Observed data.** The most spatially extensive measurements of sea ice are taken from satellites; we use two such datasets for model evaluations in this report. The first is of daily or semi-daily sea ice concentration from the NOAA Climate Data Record [17, CDR], which is derived from passive microwave observations by the Scanning Multichannel Microwave Radiometer (SMMR) and Special Sensor Microwave/Imager (SSM/I). Northern hemisphere sea ice extent is derived as the total area of the ocean covered with more than 15% ice concentration. Sea ice thickness from a processed dataset [16] has been combined into means representing Winter-Spring and Fall seasons, when the satellite laser was turned on during 2003–2008, typically for approximately 30-day periods in February/March/April and October/November. Winter and spring data were merged into a single seasonal dataset, as were the fall data, for comparison with monthly averaged model output. A more exact statistical comparison can be made using satellite emulators, which are under development as part of the E3SM project [6].

We also compare thickness will the Pan-Arctic Ice Ocean Modeling and Assimilation System (PIOMAS) data set [22], which is produced using a global coupled ocean-sea ice model that assimilates sea ice concentration and velocity, and is forced by atmospheric reanalysis data.

4.2. **Model data.** All of the models considered here evolved from the Community Earth System Model [8, CESM], including the Department of Energy's new, flagship climate model, the Energy Exascale Earth System Model [7, E3SM]. All of these simulations are fully coupled among the ocean, sea ice, atmosphere and land components, and provide state-of-the-art computer simulations of the Earth's past, present, and future climate states. Ensemble members often are created by changing air temperature by a vanishingly small amount in a single grid cell at the beginning of the simulation, and can be used to characterize uncertainty.

E3SM employs unstructured meshes, using the Model for Prediction Across Scales (MPAS) framework for ocean and ice components in version 1 (v1) and later versions. These meshes enable variable resolution for focusing computing power on fine-scale processes in particular regions of the globe, a useful feature for simulating and understanding potential navigational hazards and opportunities in the changing Arctic.

CESM is a fully coupled, global climate model which, in contrast to E3SM, runs on structured, quadrilateral ocean/ice grids and includes support for both the "low-top" Community Atmosphere Model (CAM) with its spectral element dynamical core and the "high-top" Whole Atmosphere Community Climate Model (WACCM) with stratospheric chemistry. CESM and E3SM share a common sea ice vertical physics code, Icepack [19]. We utilize CESM output produced for the Coupled Model Intercomparison Project phase 6 Diagnostic, Evaluation and Characterization of Klima experiments [4, CMIP6 DECK] as well as the Decadal Prediction Large Ensemble [12, CESM-DPLE].

The CESM DPLE consists of forty 10-year-long hindcasts (or predictions) initialized every November from 1954 to 2017. Most of our analyses utilize the first year of each ensemble, as illustrated in Fig. 1. Sea ice in this ensemble is initialized from a separate ice-ocean spinup run.

The E3SMv0-HiLAT model is very similar to CESM from which E3SM branched, but includes modifications implemented for the simulation of high-latitude processes [9]. In a previous project, we produced an ensemble of fully coupled simulations for a parameter sensitivity analysis using this model, running each simulation for 80 years in 24 present-day (year 2000) model configurations to

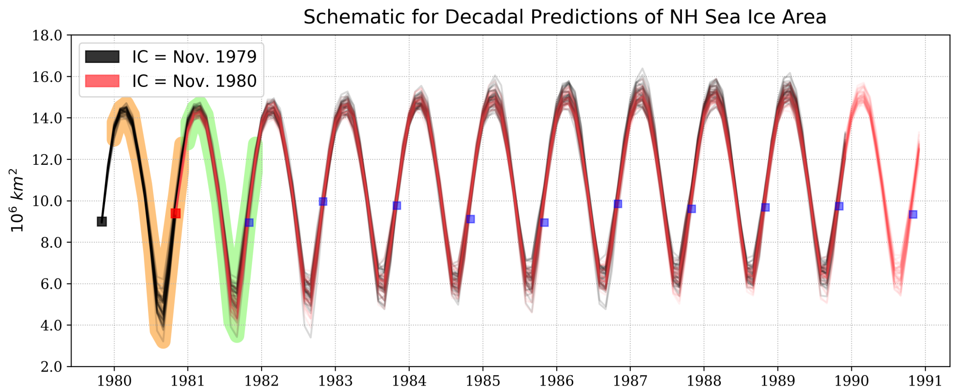

FIGURE 1. For the CESM DPLE multi-year cycle, a new, 40-member ensemble is initialized in November of each year and run for 10 years.

semi-equilibrium [25]. For the present study we analyze the model simulation that most closely represents the large-scale sea ice distribution in the Arctic.

5. Simulation results

We begin with a broad comparison across models of sea ice in the entire Arctic region, then narrow the analysis to two potential shipping corridors.

5.1. **Sea ice.** As DOE's flagship model, we use E3SM to illustrate the types of output that are generally available from all models. For example, Fig. 2 shows the sea ice extent, area, volume and snow volume simulated by the E3SM DECK ensemble, over the period 1980-2014, compared with representative data. While the E3SM is much too extensive in the winter, summer ice extent is close to observed in the earlier years, then decreases after 2007. E3SM sea ice volume also decreases in the latter half of the period and becomes less variable across the ensemble. Individual ensemble members from the same model can differ greatly, as illustrated Fig. 3.

Fig. 4 shows the average ice thickness for each model ensemble with min/max values of mean thickness in the lower right corner. E3SM exhibits greater variability than the other models during September. CESM-CAM and CESM-DPLE are much thinner than E3SM and CESM-WACCM. The difference between the CAM and WACCM configurations of CESM is primarily the inclusion of stratospheric chemistry. E3SM is too thick along the Siberian side of the Arctic in the simulations shown here; ocean eddies in a high-resolution configuration of the model improves this bias [10].

This variability is also evident in the mean annual cycles for 1980-1999 and 2000-2015 shown in Fig. 5. CESM-CAM and CESM-WACCM exhibit similar sea ice extent, with the largest differences in the summer months. E3SM has a large bias in winter, with excessive ice cover in both the Pacific and Atlantic oceans compared with data, and therefore exhibits a larger magnitude seasonal cycle. E3SM and CESM-WACCM are similarly thick in the earlier time period, with CESM-CAM much thinner; these differences decrease in the later time period.

Taylor diagrams [24] provide a more objective comparison, enabling quantification of model skill compared to reference data from observations or other models. Taylor diagrams display the standard deviation of a model ensemble along the diagram's radius and its correlation coefficient with data or another model as an angle. We compare sea ice thickness for the Arctic Ocean as in [19], which provides a minimum skill score between 0 and 1, with 1 being perfect. That score assumes perfect correlation between observationally-derived ice thickness samples, necessary

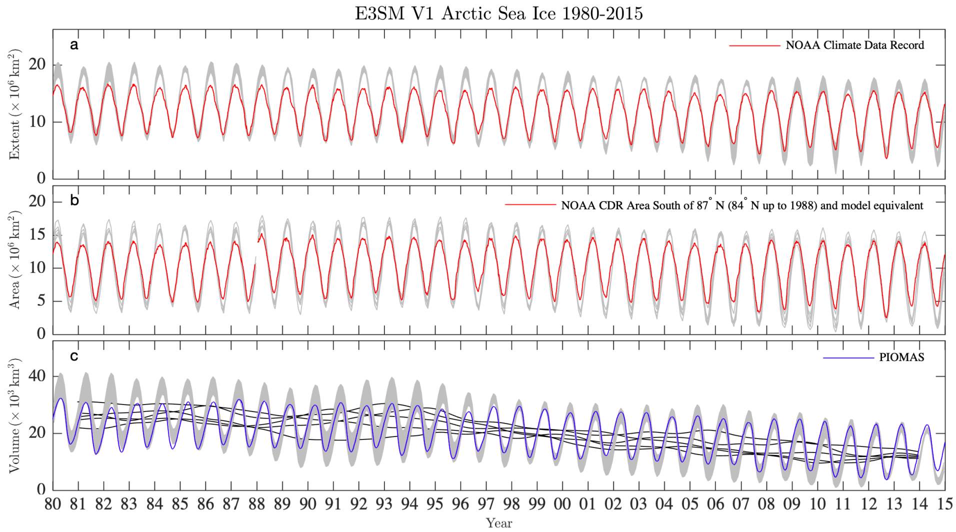

FIGURE 2. E3SM 35-year cycle compared with satellite derived observations [17] and a model that assimilates satellite data to estimate thickness [22]. The grey shading represents the range of solutions encompassed by the E3SM ensemble.

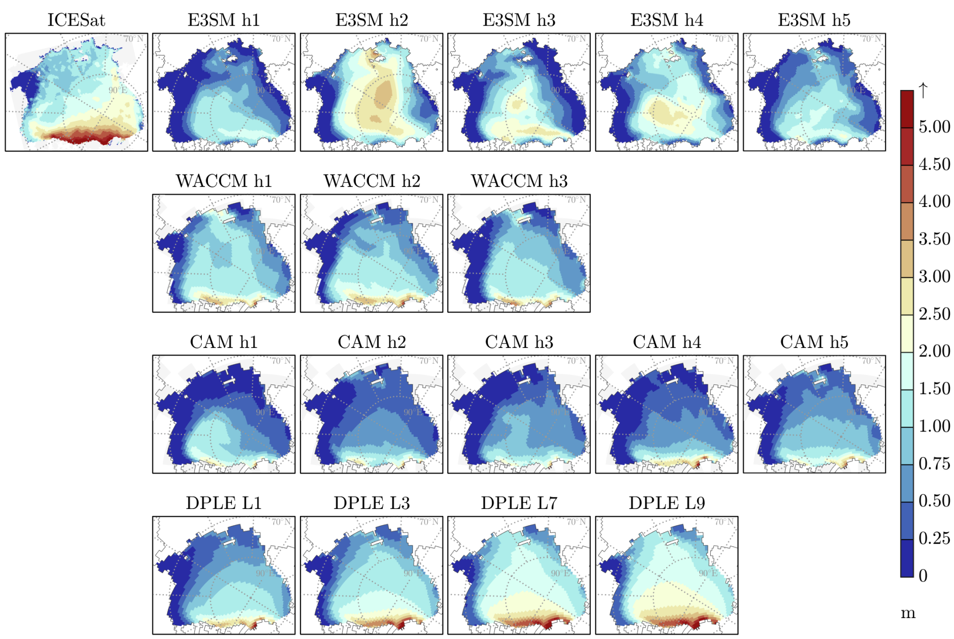

FIGURE 3. Fall season sea ice volume comparison for model ensemble members (h1, etc) compared with ICESat derived ice thickness for 2003–2008. L labels for CESM-DPLE indicate lead time in years.

because ICESat derived thickness lacks confidence bounds due to unquantifiable uncertainty in snow cover. The skill score does not indicate mean bias, which is the mean field difference between

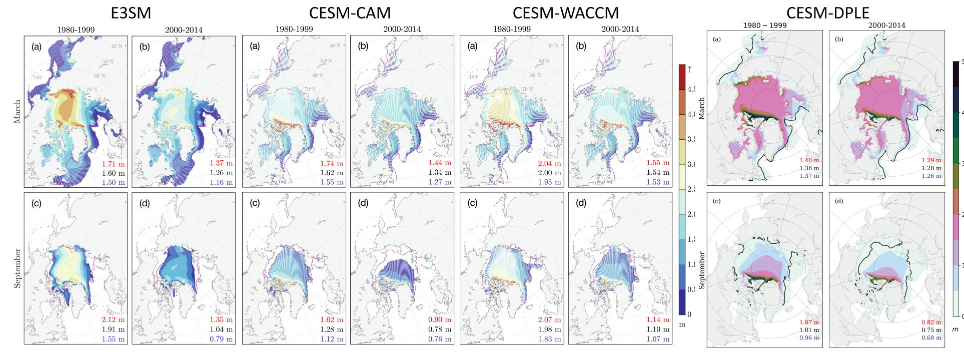

FIGURE 4. Average sea ice thickness maps for each model in March and September, 1980-1999 and 2000-2014. Min/mean/max values for each case, listed in the lower right corners, indicates the range of variability.

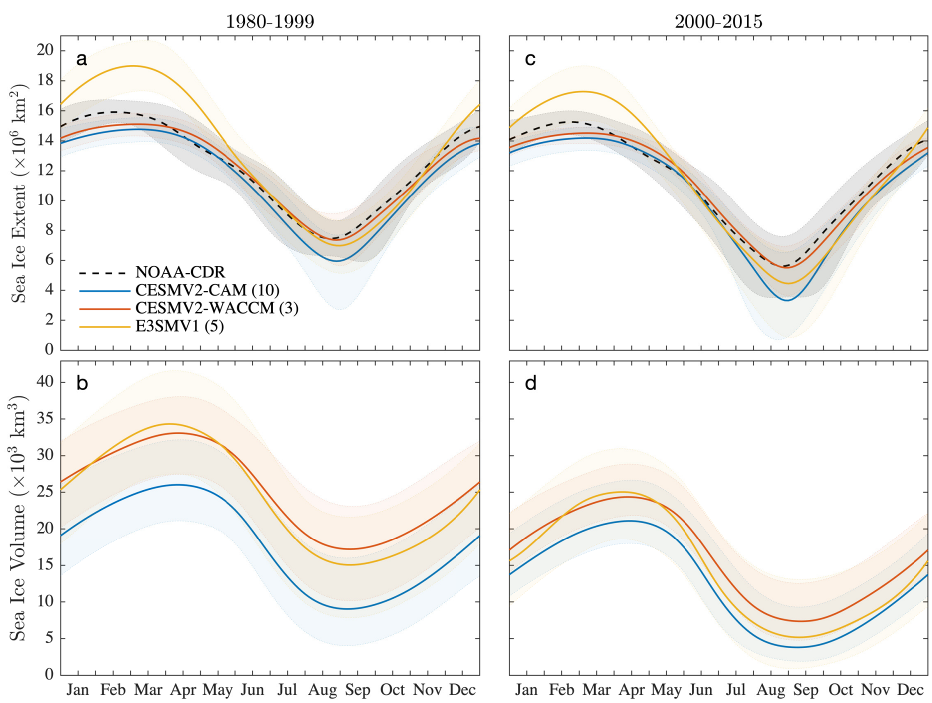

FIGURE 5. Mean annual cycles of ice extent and volume from model ensembles averaged for 1980-1999 and 2000-2015. Sea ice extent is compared with satellite data, and shading shows the envelope of ensemble members' variability.

observed and modeled ice thickness; a perfect model has zero bias. The Taylor diagrams in Fig. 6 indicate E3SM's lack of skill in this low-resolution configuration, for all ensemble members. The most skilled model is the 9-year lead-time CESM-DPLE simulation, which also exhibits small bias.

5.2. **Transportation corridors.** Fig. 7 illustrates potential transportation corridors along the Siberian coast (Northern Sea Route) and through the Canadian Archipelago (Northwest Passage), defined by the Arctic Marine Shipping Assessment [1] and used for our analysis. Equivalent tracks

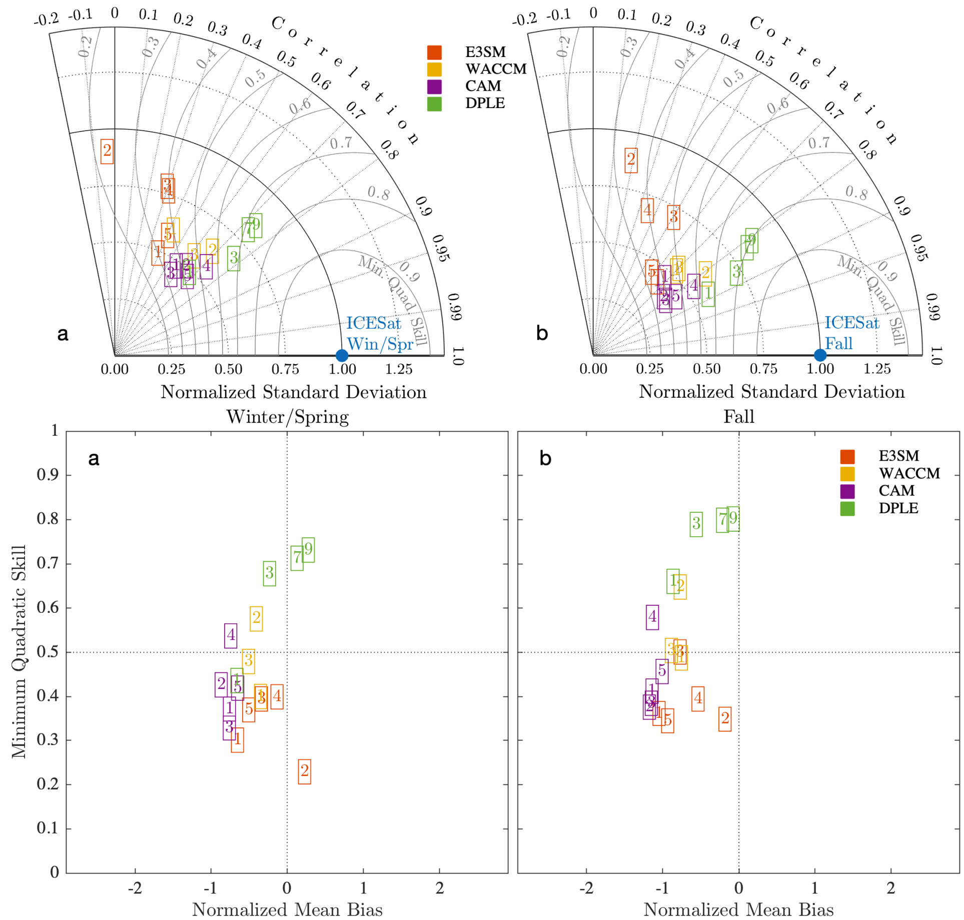

FIGURE 6. (Top) Taylor diagrams of ice thickness in the central Arctic from each model ensemble member, compared with ICESat for (left) winter/spring (right) fall. (Bottom) Arctic Ocean minimum quadratic skill versus the model's normalized mean bias for ice volume. The bias has been normalized against standard deviation. Labels correspond to ensemble members in Fig. 3.

in CESM and E3SM encounter grid cells that are defined as land in the models, and neither model's mesh allows the southern route through the Northwest Passage, which is most often traversed [11]. Models with higher resolution in high-latitude regions can mitigate this issue. Grid resolution varies from 34 to 67 km along the CESM routes and from 34 to 57 km in E3SM, illustrated in Figure 7. The grid used for HiLAT is identical to that used by CESM.

Figs. 8-9 show the sea ice concentration and thickness along the Northern Sea Route and Northwest Passage, from the model ensembles. All models produce lower values in the later time period than in the former, especially in September. The Northern Sea Route is similar for E3SM and CESM-DPLE, except for E3SM's thickness bias which is also somewhat evident in CESM-WACCM. CESM-CAM exhibits high variability while CESM-WACCM's variability is very low. CESM-CAM and CESM-WACCM both produce very thick ice in the Canadian Arctic archipelago (Fig. 9), but their variability differs. The Labrador Sea bias in E3SM is apparent; otherwise the models behave similarly in this view.

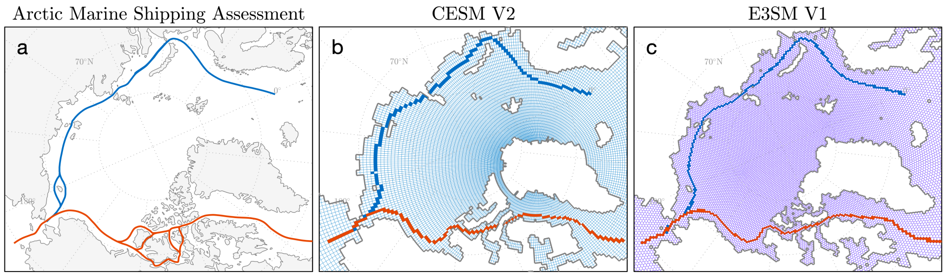

FIGURE 7. (a) Potential routes through the Northwest Passage (red) and the Northern Sea Route (blue) [1]. Equivalent tracks in (b) CESM and (c) E3SM encounter grid cells that are defined as land in the models. Green cells appear every 1000 km in (c).

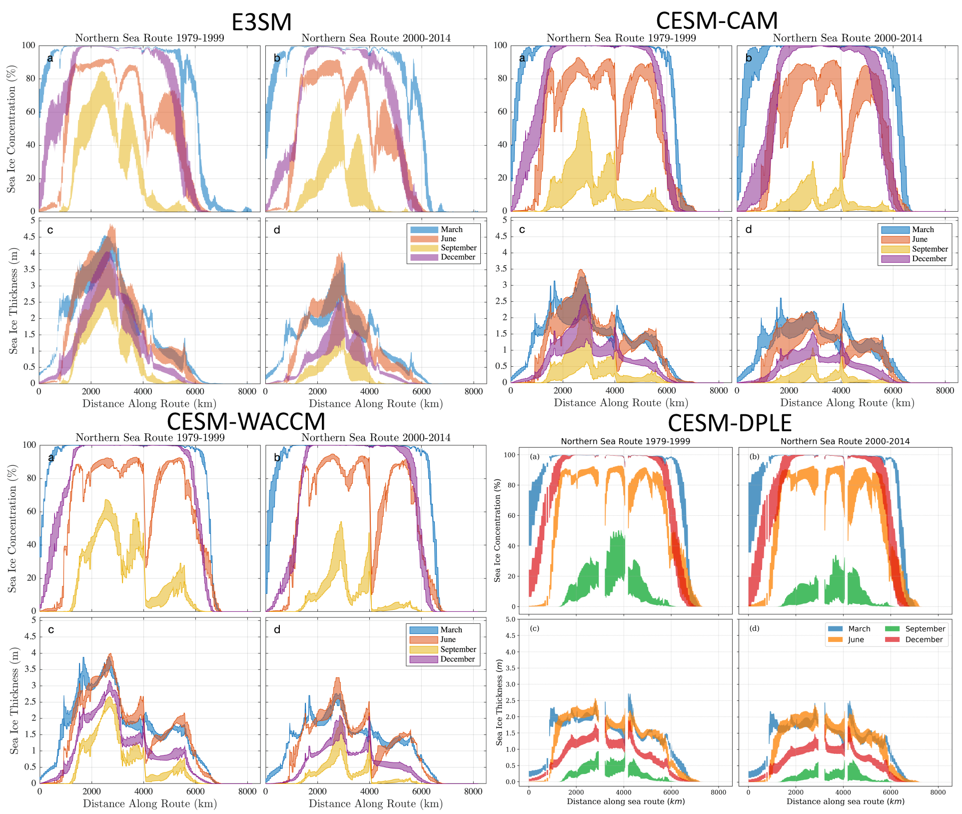

FIGURE 8. Ice concentration (upper panels for each model) and thickness (lower panels) along the Northern Sea Route, for the earlier (left) and later (right) time periods. Vertical width of the color bands, which represent different months, indicates range of variability across the ensemble members.

6. Statistical analysis of navigability

Copulas offer a means for looking at aggregated risk, particularly useful for large numbers of variables. As a proof of concept, we begin the joint probability analysis with sea ice concentration,

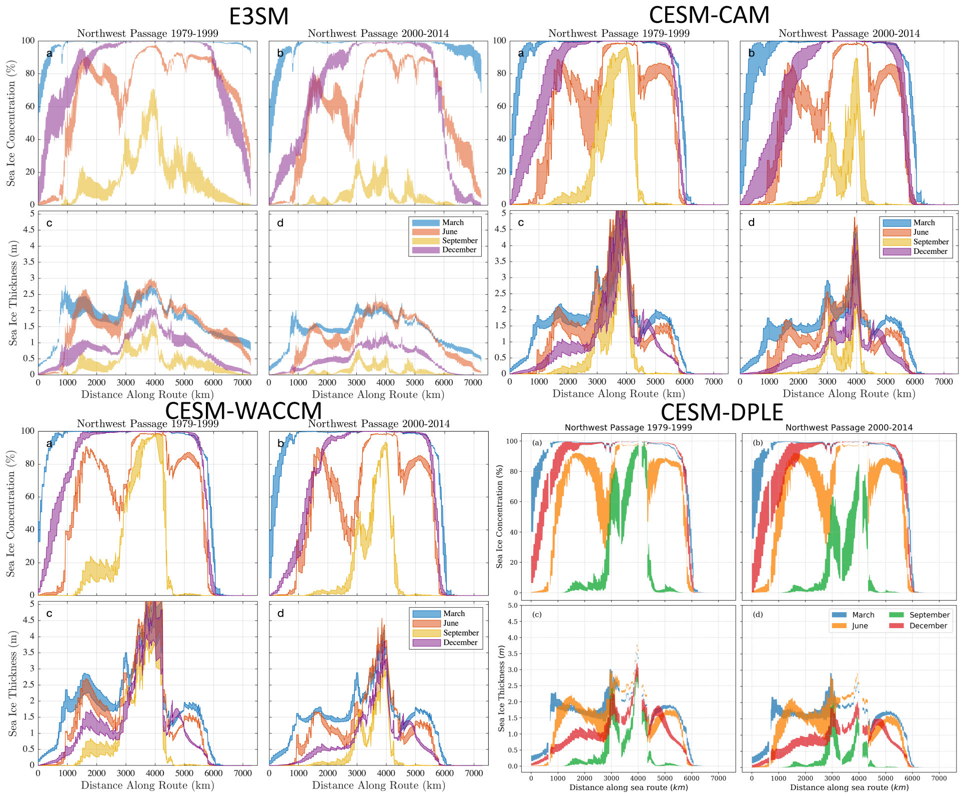

FIGURE 9. As in Fig. 8 for the Northwest Passage.

sea ice thickness and wind speed, which affects navigability directly and via the generation of waves in areas of low ice concentration. We will add air temperature and humidity to the analysis in the future, along with ridged ice area and/or volume, all of which are relevant factors for shippers.

Each of the 5826 grid cells north of 50^oN with maximum sea ice concentration greater than 15% were fit with a copula. We calculate the probability of ice concentration ≥ 0.5, ice thickness $\geq$ 1m, or wind speed $\geq$ 10m/s in each grid cell in August/September of years 51-65 for the HiLAT experiment 'EXP-01-06-06', which best captures present-day sea ice patterns (Fig. 10, left panel).[1]

Each grid cell has 30 monthly averaged records for each variable (2 months $\times$ 15 years). Distributions vary from one grid cell to another, and the flexible beta distribution is the best distribution for representing the model output data (Fig. 11). The beta distribution requires the data to lie between 0 and 1, which supports ice concentration well; thickness and wind speed were normalized by dividing by the maximum values of all the grid cells being analyzed.

Gof plots shown in Fig. 10 (middle) indicate that the beta distribution fits the concentration, thickness and wind speed data well. The quantile-quantile (Q-Q) plot helps us assess whether a data set plausibly came from some theoretical distribution; if so, the points form a roughly straight line. The probability–probability or percent–percent (P–P) plot is used to assess how closely two data sets agree, by plotting the empirical and theoretical cumulative distribution functions (CDF) against each other. Gof tests indicated that beta distribution was rejected for about 13% of grid

[1]September data from year 53 were corrupted and not used.

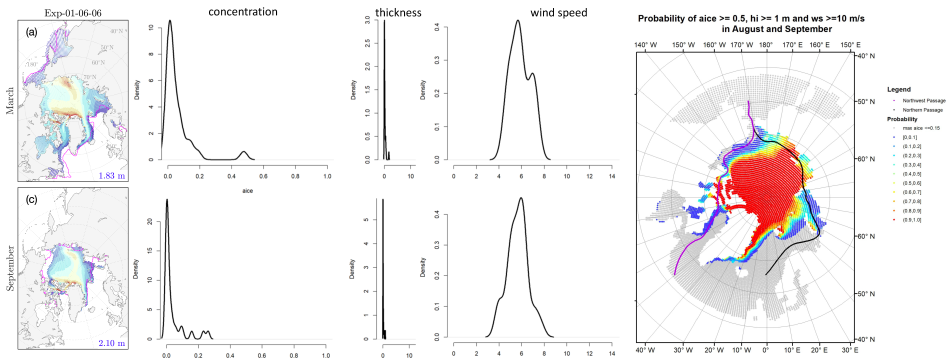

FIGURE 10. (Left) HiLAT maps as in Fig. 4 for a single ensemble member. (Middle) Beta distribution fit for ice concentration, thickness and wind speed in grid cell (1, 366) for the (upper) model and (lower) copula emulation. (Right) Probability of sea ice being more than 50% concentration, or more than 1 m thick, or experiencing wind speeds greater than 10 m/s during August and September of years 51-65.

cells for concentration, 2% for thickness and none for wind speed. Most of the rejections were grid cells with dominantly zero values.

The gof tests were then used to choose a copula to be fitted to the data, which can be different from one grid cell to the next. Copula options include Clayton (MTCJ), Gumbel, t, Frank, Normal (Gaussian), Joe. Where gof tests failed, a copula was chosen randomly. The fitted copula is then used to generate random numbers for the distribution. Fig. 12 compares the copula-simulated probability distribution functions for concentration, thickness and wind speed with the original model output, for grid cell (1, 366). The joint probability density function and cumulative distribution function of the variables are then found, and the probability of the variables jointly obtaining values beyond certain thresholds can then be calculated. This procedure is executed for each grid cell, resulting in a map such as Fig. 10 (right panel) showing the probability of encountering sea ice concentration at least 50%, or thickness at least 1 m, or wind speed $\geq$ 10m/s.

Wind speed and waves are important factors in navigability that are not accounted for in standard sea-ice based metrics, and need to be treated independently due to variations in fetch in regions with sea ice [20]. Our analysis can be extended for more variables using the same procedure. For instance, air temperature and humidity could be added to assess risk of ship superstructure icing in areas where ice concentration and thickness is low enough that ships might be present.

7. Discussion and conclusions

With a long history of Arctic research, Los Alamos has expertise in ocean, sea-ice, and atmospheric physics and uncertainty quantification, global and regional modeling, and a wealth of Earth system simulations available for analysis. The goal of this project was to use those simulations to characterize physical properties and uncertainties in the Arctic relevant to ocean acoustics, hazardous weather conditions, and navigable shipping corridors, and to assess the quality of Department of Energy (DOE) simulations for national security use. In addition, this research provides a baseline to articulate future model development needs for DOE Office of Science.

We evaluated several models' representations of sea ice conditions in the Arctic against observational data and evaluated a multivariate approach for assessing risk due to both sea ice and atmospheric conditions. While fully coupled simulations are not tied to particular time periods,

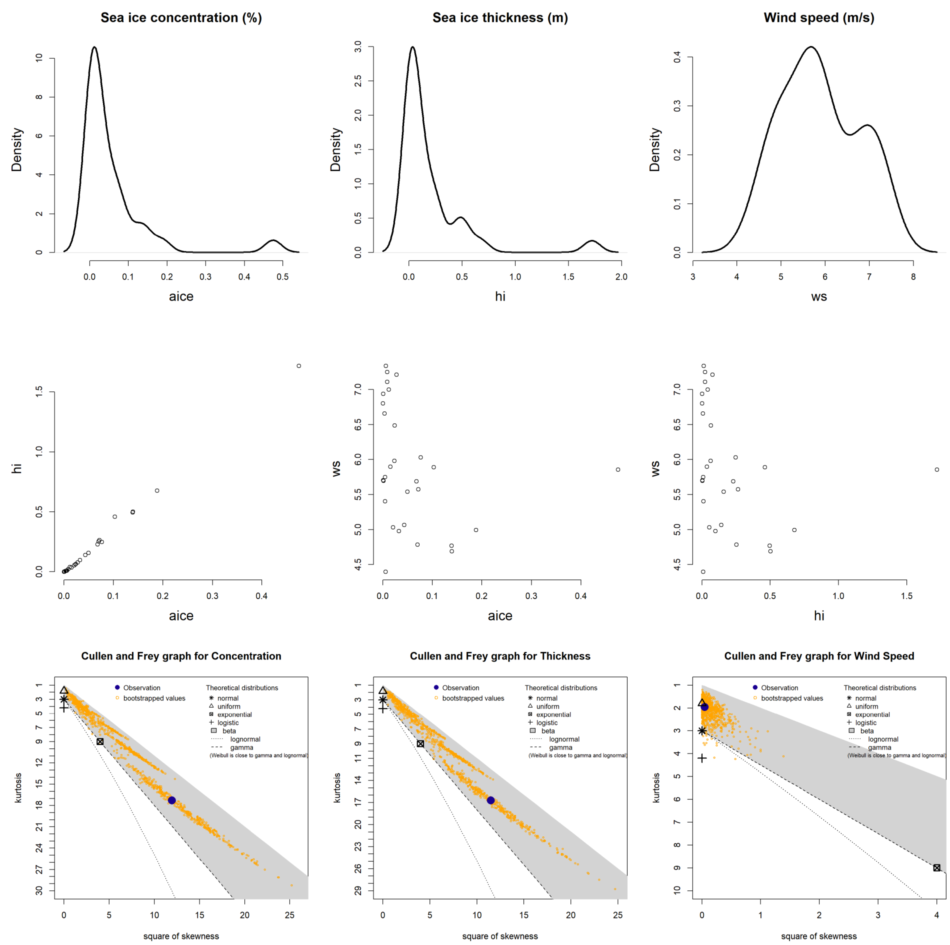

FIGURE 11. (top) Probability distribution functions for ice concentration, thickness and wind speed in a sample grid cell, EVH0 (1, 366). (middle) Scatter plots of the three variables. (bottom) Cullen and Frey graphs indicates that the beta distribution fits the data better than the other available distributions.

the CESM-DPLE effort ameliorates this problem by reinitializing the ensemble each year using ocean and sea ice output from another run forced by atmospheric reanalysis data for particular dates. Ensembles of model simulations sample the range of variability attainable by each model and may not capture the full range of potential uncertainty. It is not clear why CESM-WACCM shows much less variation than the other model configurations, but we can surmise that its stratospheric aerosol forcing exerts a very strong influence. Statistical measures are necessary to capture and characterize the uncertainty inherent in the physical and model systems. A major issue with statistical approaches for climate study is that the base data are nonstationary as the climate changes; this project does not attempt to address this issue.

In general, the climate ensembles evaluated here lack skill for short-term, detailed operational use, although CESM-DPLE shows promise. Its improved skill is likely associated with the manner in which the sea ice and ocean components are reinitialized each year. Understanding why the 9-year lead-time simulations outperform those with shorter lead times requires additional work; we hypothesize that the initialized field is too thin and growth over time brings it closer to observations.

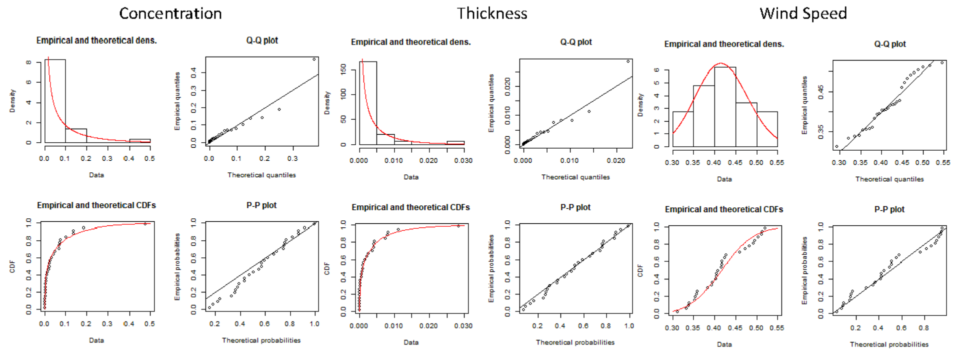

FIGURE 12. Beta distribution fit for ice concentration, thickness and wind speed in grid cell (1, 366). The histograms and diamonds are the model output; the solid lines show the fitted distribution function.

The other models also capture essential physical processes and show some skill, though biased. Model initialization is key.

A common approach for evaluating and communicating navigability through areas of sea ice is the Ice Numeral, which is tailored to particular classes of ships [2]. Because we have most of the sea ice variables needed for the estimates, or close proxies, our model data can be used to estimate the Ice Numeral from climate simulations. Table 1 lists existing model variables needed for the Ice Numeral and potential proxies for those that are missing or defined differently. Our estimates would be conservative, e.g. ignoring the possibility of weak, rotten ice would enhance the safety margin. In the future, a statistical framework using copulas could be used to combine relevant variables into joint probability distributions, creating a new, extended metric for ice navigability

TABLE 1. Quantities used to calculate Ice Numeral in operational settings [2], and potential equivalents in the sea ice model CICE. Most variables are typically available as grid-cell means, but individual category values (n) could be saved and used for finer resolution.

Canadian Ice Service variable	CICE variable	Notes
Ice concentration	aice(n)	fractional ocean surface coverage
Thickness-based development stages	hi(n)	use *actual* ice thickness
Age-based development stages	iage	use chronological age
	FYarea	or 1st-year ice area (complement)
	hi	or assume ice $>$ 2 m is older
Icebergs	not available	under development (E3SM)
Stages of decay		
no melt	melt[b,t,l]	meltb+meltt+meltl=0
snow melt	melts	melts ≥ 0
ponding	apnd	if melt ponds on, check apnd > 0
	meltt	if melt ponds off, check meltt $\neq 0$
thaw holes	not available	compare pond depth with ice thickness
Ice roughness	aice(n), ardg(n)	increment IN if aicen>0.6 and ardgn>1/3

that includes atmosphere and ocean conditions not currently considered. Users would still need to consider their vessel limitations.

7.1. **Technical challenges and considerations.** Sea ice modelers typically only show ice quantities in grid cells with more than 15% ice coverage, because observed data is less reliable. This cutoff value may need to be reconsidered for operational uses, particularly when considering atmospheric variables that worsen with decreasing sea ice coverage, such as icing from sea spray. Likewise, climate models typically output only grid-cell-mean ice thickness, rather than the actual ice thickness of the portion of the grid cell that is covered with ice. Actual thickness can be computed from the mean fields, but this introduces errors due to averaging. A related issue is lack of uncertainty information for ice thickness in satellite derived thickness data. Nonstationarity inherent in climate change, and incorporating information quantifying disagreement among observational products, also pose challenges.

Copula analysis worked well for most grid cells with sea ice although it failed in a few cells, primarily where there was often no ice. Assigning risk for multiple variables requires assigning cutoff values for each, and the appropriate cutoff may depend on the particular problem, e.g. the vessel being used.

Potential US sponsors of this work are interested in the Northwest Passage, but models generally perform better for the Northern Sea Route, partly due to the resolution needed among the Canadian islands. Low-resolution meshes can not resolve narrow waterways, and we found that land blocks the primary Northwest Passage routes in our models. This issue is now being remedied by E3SM.

Arctic ocean simulations are generally poor below 250m [14], although newer E3SM simulations show improvement. Three-dimensional ocean analyses may be done in future work with E3SM.

7.2. **Recommendations.**
DOE climate projects: Use CMIP6 conventions for sea ice model output, and in particular, output actual ice thickness in addition to grid-cell-mean values. When creating new meshes, check the representation of narrow passages in the Canadian Arctic for future analyses. Collaborate to develop standardized tools suitable for model output analysis in high latitudes.
Observing systems: Provide uncertainty bounds for ice thickness.
Extending this project: Compare atmospheric variables with data. Apply the copula analysis to other models, particularly CESM-DPLE and E3SM. Work with the National Ice Center to compare and validate a model based Ice Numeral with their version, then extend it to include multiple variables using copulas. Develop metrics to evaluate sea ice degradation in models. Evaluate ocean model output in the Arctic in E3SM.

7.3. **Transition directions.** This project is helping to define requirements for E3SM's MPAS-Analysis tools for high-latitude use, which are currently insufficient for this project due to sampling times and other issues. We expect that our analysis toolbox will be developed into a standard tool (possibly python) usable across projects; one of the BER program managers (Joseph) has already expressed interest in funding such an effort. The metrics described here could prove useful for a new, Arctic coastal project successfully proposed to DOE/BER after this project began. The National Geospatial Intelligence Agency is interested in follow-on research to further develop these capabilities for E3SM, which has been ported to a classified computer system as part of a separate, internally funded LANL project. An important step will be working with the National Ice Center to validate the new metric.

8. Supplemental project information

8.1. Project products.
Poster: "Impacts of an Ice-Diminishing Arctic on Naval and Maritime Operations" conference, Washington DC, Jul 2019
Talk: "Defining a cutting-edge future for sea ice modelling" workshop, Iceland, Sep 2019
Talk: Interagency environmental security visitors, Los Alamos National Laboratory, Sep 2019
Manuscript: "Diagnosing Near-Future Changes in Arctic Sea Ice and Ocean Conditions", in prep. This paper primarily requires additional reference to existing research on Arctic shipping routes.

8.2. Project management challenges. The original proposal team included staff members and one postdoc with expertise across the various models along with particular interests in uncertainty quantification. Two staffing challenges quickly became apparent: staff were already overcommitted on their other projects, and the postdoc who proposed the copula analysis finished his term at LANL and moved away. Also, the multi-model CMIP5 data sets were too big and unwieldy to deal with in such a short project; CMIP6 ensemble members are still being run for future forcing scenarios, which have only recently been defined; and there was no single set of analysis tools suitable for use with all models. In response to these issues, we restricted the models used to those with which our team was already familiar, which are all based on CESM; we added several people to the project; and we replaced the multi-model CMIP6 output with NCAR's Decadal Prediction Large Ensemble.

Climate model data sets are extremely large and often analyzed in situ on the machines on which they are run. Since our team is made up of project staff from several different modeling efforts, we did not all have access to every platform and all data. We utilized LANL's free data storage, extracting just those variables we expected to need. Access/permission to this resource was a problem for Mac and PC, but we were able to set up a second storage area accessible to both. Also, many of our local workstations were configured incorrectly, prevented access until fixed.

We attempted to unify our analysis using an existing set of Matlab scripts, and found that LANL does not have a site-wide Matlab license. The license owned by CCS division does not have all of the supplemental packages that we needed, and competition for licenses with other CCS users prevented progress for this project. We therefore bought an individual license for one team member, who then carried much of the responsibility for creating plots.

9. Acknowledgments

We thank the Laboratory Directed Research and Development Office for funding this work, and we acknowledge the supercomputing resources provided by DOE/NERSC, NSF/CISL/Cheyenne and LANL Institutional Computing for the simulations analyzed herein. The CESM project is supported primarily by the National Science Foundation (NSF); computing and data storage resources for the CESM ensembles, including the Cheyenne supercomputer (doi:10.5065/D6RX99HX), were provided by the Computational and Information Systems Laboratory (CISL) at NCAR. We thank all the scientists, software engineers, and administrators who contributed to the development of E3SM, CESM2, and E3SMv0-HiLAT. We are also grateful to Dr. Rachel Bernstein and Cmdr. Kelly Taylor of the National Geospatial Intelligence Agency for inspiration.

References

[1] Arctic Council. Arctic Marine Shipping Assessment. Technical report, 2009. Second printing.

[2] Canadian Ice Service. Arctic Ice Regime Shipping System. Technical Report TP 14044E, Transport Canada, 2003.

[3] CICE Consortium. CICE and Icepack software, cited 2019. Available online at http://github.com/CICE-Consortium.

[4] Coupled Model Intercomparison Project. CMIP6 Diagnostic, Evaluation and Characterization of Klima (DECK) experiments, cited 2019. [Available online at https://www.wcrp-climate.org/wgcm-cmip/wgcm-cmip6].

[5] Department of Defense. Report to Congress on Strategy to Protect United States National Security Interests in the Arctic Region. Technical Report A-CE2489B, Department of Defense, 2016.

[6] A. F. Roberts et al. Evaluating Coupled Sea Ice Models using an Altimetric Satellite Emulator. 2019. In prep.

[7] C. Golaz et al. The DOE E3SM Coupled Model Version 1: Overview and evaluation at standard resolution. *Journal of Advances in Modeling Earth Systems*, 11(7):2089–2129, 2019.

[8] J. W. Hurrell et al. The Community Earth System Model: A framework for collaborative research. *Bull. Amer. Meteor. Soc.*, 94(9):1339–1360, 2013.

[9] M. Hecht et al. E3SMv0-HiLAT: A modified climate system model targeted for the study of high-latitude processes. *Journal of Advances in Modeling Earth Systems*, 0(0), 2019.

[10] P. M. Caldwell et al. The DOE E3SM coupled model version 1: Overview and evaluation at standard resolution. *Journal of Advances in Modeling Earth Systems*, 2019. Submitted.

[11] R. K. Headland et al. Transits of the Northwest Passage to end of the 2018 navigation season, Atlantic Ocean – Arctic Ocean – Pacific Ocean. Technical report, Scott Polar Research Institute, 2018. Revised 1 Dec 2018.

[12] S. G. Yeager et al. Predicting near-term changes in the Earth system: A large ensemble of initialized decadal prediction simulations using the community earth system model. *Bull. Amer. Meteor. Soc.*, 99(9):1867–1886, 2018.

[13] J. W. Greenert. The United States Navy Arctic Roadmap for 2014 to 2030. Technical Report ADA595557, Office of Chief of Naval Operations, 2014.

[14] Alexandra Jahn, Kara Sterling, Marika M. Holland, Jennifer E. Kay, James A. Maslanik, Cecilia M. Bitz, David A. Bailey, Julienne Stroeve, Elizabeth C. Hunke, William H. Lipscomb, and Daniel A. Pollak. Late-twentieth-century simulation of arctic sea ice and ocean properties in the ccsm4. *Journal of Climate*, 25(5):1431–1452, 2012.

[15] C. Kinnard, C M Zdanowicz, D A Fisher, E Isaksson, A de Vernal, and L G Thompson. Reconstructed changes in Arctic sea ice over the past 1,450 years. *Nature*, 479(7374):509–512, 2011.

[16] Ronald Kwok and G F Cunningham. ICESat over Arctic sea ice: Estimation of snow depth and ice thickness. *Journal of Geophysical Research-Oceans*, 113(C8), 2008.

[17] Walter N. Meier. Climate Data Record (CDR) Program Climate Algorithm Theoretical Basis Document (C-ATBD) Passive Microwave Sea Ice Concentration. Technical Report CDRP-ATBD-0107, National Oceanic and Atmospheric Administration, 2013.

[18] National Intelligence Council. Implications for US National Security of Anticipated Climate Change. Technical Report NIC WP 2016-01, U.S. Government, 2016.

[19] A. F. Roberts, E. C. Hunke, R. Allard, D. A. Bailey, A. P. Craig, J.-F. Lemieux, and M. D. Turner. Quality control for community-based sea-ice model development. *Phil. Trans. Roy. Soc. A*, 376(2129):20170344, 2018.

[20] E. M. Samuelsen. Ship-icing prediction methods applied in operational weather forecasting. *Quarterly Journal of the Royal Meteorological Society*, 144(710):13–33, 2018.

[21] C. Scholzel and P. Friederichs. Multivariate non-normally distributed random variables in climate research — Introduction to the copula approach. *Nonlin. Proc. Geophys.*, 15:761–772, 2008.

[22] A. Schweiger, R. Lindsay, J. Zhang, M. Steele, and H. Stern. Uncertainty in modeled arctic sea ice volume. *J. Geophys. Res.*, 2011.

[23] S. R. Stephenson, L. C. Smith, and J. A. Agnew. Divergent long-term trajectories of human access to the Arctic. *Nature Climate Change*, 1:156 EP –, 05 2011.

[24] K. E. Taylor. Summarizing multiple aspects of model performance. *Journal of Geophysical Research*, 106(D7):7183–7192, 2001.

[25] J. Urrego-Blanco, E. Hunke, and N. Urban. Emergent relationships among sea ice, longwave radiation and the Beaufort High circulation exposed through parameter uncertainty analysis. *J. Geophys. Res. Oceans*, 2019. Accepted.